ARTICLE

Phase Inversion in Polylactide/Soybean Oil Blends Compatibilized by Poly(isoprene-*b*-lactide) Block Copolymers

Kwanho Chang, Megan L. Robertson, and Marc A. Hillmyer*

Department of Chemistry, University of Minnesota, Minneapolis, Minnesota 55455

ABSTRACT Renewable composites were prepared by melt blending of polylactide and soybean oil. The blend morphology was tuned by the addition of poly(isoprene-*b*-lactide) block copolymers. Due to the extreme difference in the viscosities of soybean oil and polylactide, a critical block copolymer composition was found to induce a phase inversion point at which the minor soybean oil phase became the matrix surrounding polylactide particles. This transition was due to the thermodynamic interactions between the block copolymer and the two phases and shear forces acting on the mixture during blending. The size of the soybean oil droplets in the polylactide matrix was also highly dependent on the block copolymer composition. In binary polylactide/soybean oil blends, there was a limiting concentration of soybean oil that could be incorporated into the polylactide matrix (6% of the total blend weight), which could be increased up to 20% by the addition of block copolymers.

KEYWORDS: renewable resource polymers • phase inversion • polylactide • soybean oil • block copolymer compatibilization • polymer blends

INTRODUCTION

In recent years, there has been an increasing emphasis on finding alternatives to replace traditional nondegradable petroleum-based plastics. Of great interest and environmental importance are renewable feedstocks for polymeric raw materials (1−5). Polylactide is one of the most extensively studied polymers derived from an annually renewable resource because of its biocompatibility and biodegradability for biomedical applications as well as its competitive physical properties (6−8).

The broad application of poly(L-lactide) (PLLA) as a commodity polymer has been limited because of its brittle nature. Many approaches have been taken to develop toughening agents for increasing the impact strength of PLLA (9). The effects of the polymer stereochemistry, processing history, and addition of plasticizers have all been studied (9). In addition, PLLA has been blended with nondegradable, nonrenewable materials such as polyethylene (10), polyurethanes (11), and poly(ethylene oxide) (12) with significant improvements in the tensile toughness and impact strength. Biodegradable blending partners have also been explored, with much emphasis on the use of poly(ε-caprolactone) (13). There are fewer examples in the literature of renewable toughening agents for PLLA. However, blends of PLLA with poly(hydroxyalkanoates) (14), microbially derived polymers, and the partially renewable poly(butylene succinate) (15) have been explored. Recently, moderate improvements in the elongation at break of PLLA were gained by the addition of epoxidized soybean oil (16). In the past, soybean oil and epoxidized soybean oil have been blended with other degradable and/or renewable polymers such as poly(3-hydroxybutyrate-*co*-3-hydroxyvalerate) (17) and poly(L-lactide-*co*-caprolactone) (18). The challenge remains to find a completely renewable and biodegradable toughening agent that when blended with PLLA, will result in similar properties that are obtained with nonrenewable and nonbiodegradable modifiers.

The focus of this paper is to utilize annually renewable and biodegradable vegetable oils as blending partners for PLLA. The derivation of new materials from vegetable oils has been a subject of much interest in the literature (19−21). A vegetable oil is a mixture of triglycerides with varying degrees of unsaturated fatty acids. Among the family of vegetable oils, of particular interest is the use of soybean oil (SOY) because of its abundance and low cost. The production of SOY is slightly greater than 30% of the global production for all vegetable oils (22). Around 84% of fatty acids in SOY are oleic, linoleic, and linolenic acids possessing 4.6 nonconjugated C═C bonds on average per triglyceride molecule (21), which allows for the reaction with other monomers and chemical modification such as epoxidization, maleinization, and acrylation (19−21). In this article, SOY is used as a raw material without chemical modification.

The mechanical properties of blends of immiscible materials are highly dependent on the morphology. In blends consisting of droplets of one component incorporated into a matrix of the second component, key parameters are the particle size of the dispersed phase and the matrix ligament thickness, which is the distance between the droplets. The impact strength of an immiscible polymer blend, which is a measure of the material toughness, is dependent on one or

* Corresponding author. E-mail: hillmyer@umn.edu.
Received for review August 4, 2009 and accepted September 20, 2009
DOI: 10.1021/am900514v

Published on Web 10/02/2009

both of these parameters, depending on the nature of the matrix polymer (23−25).

In the present study, the morphologies of PLLA/SOY blends are probed. Many parameters affect the blend morphology such as the interfacial tension between the two phases, blend composition, blend preparation technique such as solvent casting or melt mixing, and ratio of the viscosities of the two phases (26, 27). The final blend morphology can also be greatly affected by droplet coalescence (28, 29). Blending two materials with highly different viscosities leads to additional challenges because there is a fundamental limit on the volume fraction of the less viscous component (SOY) that can be distributed in the more viscous matrix (PLLA). Phase inversion in a binary mixture, beyond which the dispersed minority phase droplets are converted into a continuous phase, can be approximated by a simple empirical equation given by

$$\frac{\varphi_A}{\varphi_B}\frac{\eta_B(\dot{\gamma}, T)}{\eta_A(\dot{\gamma}, T)} \cong 1 \qquad (1)$$

where φ_i is the volume fraction and η_i is the viscosity of each component i at a shear rate $\dot{\gamma}$ and temperature T, respectively (30). Phase inversion is expected when the volume fraction ratio approaches the viscosity ratio. Equation 1, originally developed for binary polymer blends with closely matched viscosities, has been modified to describe blends with more disparate viscosities (30). Phase inversion has been documented in several binary homopolymer blends in the quiescent condition and under shear (31−33). The viscosities of PLLA and SOY differ by roughly 5 orders of magnitude, and thus it is expected that phase inversion could occur at a very low level of SOY.

Due to the immiscibility of PLLA and SOY, as determined in this study, we used a block copolymer [poly(isoprene-*b*-lactide) (ILLA)] as a blend compatibilizer. We show that the Flory−Huggins interaction parameter, χ, between SOY and polyisoprene (PI) is small enough to result in miscibility between the PI block and SOY domains. The effect of the block copolymer composition on the interfacial tension of a system of two A/B immiscible polymers and the corresponding A-*b*-B diblock copolymer has been previously studied (34, 35). In ref 34, self-consistent-field theory (SCFT) calculations showed that there is a balance point in terms of the block copolymer composition at which the saturated block copolymer monolayer at the homopolymer interface has a zero spontaneous curvature. At this balance point, the interfacial tension becomes vanishingly low. Moreover, the interfacial tension (a sensitive function of molecular parameters such as the molecular weight of each component, Flory−Huggins interaction parameter χ, and statistical segment lengths of monomer segments) parabolically increases as the block copolymer composition begins to deviate from the balanced composition. We show that the composition of the block copolymer is a key parameter for controlling the morphology of PLLA/SOY/ILLA blends and also for the suppression of phase inversion in these blends.

In this paper, we discuss the morphology of PLLA and SOY blends prepared by melt mixing and compatibilization with ILLA block copolymers. The Flory−Huggins interaction parameters for all of the blend components are characterized by cloud-point measurements. We find that phase inversion in the compatibilized blends is dependent not only on the presence of shear forces during mixing but also on the block copolymer composition.

EXPERIMENTAL DETAILS

Synthesis and Characterization of Blend Components. Wesson soybean oil (SOY) was purchased in a local grocery store and used without further purification. The poly(L-lactide) (PLLA) homopolymers were synthesized by ring-opening polymerization of L-lactide (36). L-Lactide (Aldrich) was recrystallized from ethyl acetate before use. In a glovebox, 1.0 M L-lactide was dissolved in toluene in a high-pressure vessel with a 1:2 mole mixture of triethylaluminum ($AlEt_3$) and benzyl alcohol. After it was tightly sealed with a Teflon cap, the vessel was transferred to an oil bath outside of the glovebox at 90 °C and heated with stirring for 3 h. The reaction was terminated with acidic water, vigorously washed with distilled water, and purified through a silica column. After concentration in a rotary evaporator, residual solvent was removed by drying in a vacuum oven at 80 °C for 3 days. A typical lactide conversion was about 80%. For melt blending in a DACA mixer, commercial-grade PLLA was supplied as pellets by Toyota Motor Corp. The polyisoprene (PI) homopolymers were synthesized by anionic polymerization. Isoprene monomer (Aldrich) was purified by sequential distillation from calcium hydride at room temperature and *n*-butyllithium (Aldrich) twice at 0 °C. The reaction was initiated with *sec*-butyllithium (Aldrich), carried out in cyclohexane at 40 °C for 6 h under an argon atmosphere, and terminated with degassed acidic methanol.

Poly(isoprene-*b*-lactide) (ILLA) block copolymers were synthesized by a combination of anionic and ring-opening polymerization (37). Hydroxyl-terminated PI (PI−OH) was prepared as a macroinitiator using anionic polymerization. The PI living chains, which were synthesized in a 1 L reactor as described above, were end-capped with excess 50 M ethylene oxide (Aldrich) that had also been purified over calcium hydride for 4 h at 0 °C. After stirring at room temperature for an additional 12 h, the reaction was terminated with acidic methanol. Once completely dried in a vacuum oven for 3 days, PI−OH was used to synthesize a series of ILLA block copolymers with different block compositions by attaching varying amounts of L-lactide using the procedure described above. The polymerization was quenched with 2 N acidic water after 6−12 h of reaction time (75−80% conversion) depending upon the concentration of $AlEt_3$ and precipitated in a 3:1 by volume mixture of methanol/isopropyl alcohol.

The number-average molecular weight (M_n) of the homopolymers and the fraction of 1,4 regioisomer (>93%) in the PI homopolymers were determined from ^{1}H NMR spectroscopy. The polydispersity index (PDI = M_w/M_n, where M_w is the weight-average molecular weight) was measured using a Hewlett-Packard 1100 series size-exclusion chromatograph equipped with a Hewlett-Parkard 1047A refractive index detector using chloroform as the mobile phase at 35 °C. The characteristics of the block copolymers are listed in Table 1. The block copolymer composition f_{PLLA} was determined from ^{1}H NMR spectroscopy. All of the block copolymers in Table 1 have the same PI block (M_n = 5900 g/mol and PDI = 1.08). The commercial PLLA pellets supplied by Toyota had the following characteristics: M_n = 54 kg/mol and PDI = 1.73, both of which were measured based on size-exclusion chromatography (SEC) data using polystyrene standards. For all other polymers dis-

Table 1. Material Characteristics of Block Copolymers[a]

sample	M_{PLLA} (kg/mol)	PDI	f_{PLLA}
ILLA42	5.9	1.12	0.42
ILLA53	9.1	1.10	0.53
ILLA55	10.0	1.11	0.55
ILLA59	11.7	1.13	0.59
ILLA62	13.1	1.13	0.62
ILLA63	14.2	1.13	0.63
ILLA66	16.1	1.16	0.66
ILLA70	19.1	1.18	0.70
ILLA74	22.7	1.18	0.74
ILLA80	33.2	1.24	0.80

[a] M_{PLLA} = number-average molecular weight of the PLLA block, PDI = polydispersity index, and f_{PLLA} = volume fraction of PLLA in ILLA at 190 °C.

cussed in this paper, an absolute molecular weight is reported. Molecular characteristics of the homopolymers used in cloud-point measurements are given in the Supporting Information.

Blend Preparation. Melt blends were prepared by loading 4.0 g of the total sample in a DACA batch twin-screw mixer. The blend components were continuously circulated by tapered twin screws through a channel. The mixing torque and normal force were read by a transducer positioned below the chamber. The PLLA homopolymer (Toyota) was dried overnight in an oven at 80 °C before blend preparation. Typical blend protocols are as follows. The mixing speed and temperature were set to 100 rpm and 190 °C unless otherwise stated. In the case of binary blends, PLLA pellets were initially homogenized for 3 min under a nitrogen purge. Then SOY was added dropwise using a glass pipet. For ternary blends, dry mixtures of PLLA/ILLA were injected together and preblended for 5 min before the addition of SOY. After 20 min, the blends were extruded and immediately quenched in liquid nitrogen to preserve morphology.

Additional binary and ternary blends were prepared by solvent-casting. A total of 1.0 g of sample was dissolved at 10 wt % in chloroform and cast onto Petri dishes. After 3 days, the residual solvent in the blends was further dried at 60 °C in a vacuum oven for 1 day. These samples were annealed in vacuum-sealed glass ampules for morphology observation or hot-pressed at 190 °C into disks with a diameter of 25 mm and a thickness of 1.0 mm for dynamic mechanical analysis.

Determination of the Concentration of SOY in Binary and Ternary Blends. A calibration curve was prepared by analysis of the SEC data of PLLA and SOY blends with known concentrations. The relative peak areas of PLLA and SOY at each concentration were determined, and the ratio of the PLLA peak area to the SOY peak area was plotted as a function of the SOY concentration. For a binary or ternary blend of unknown SOY concentration, the relative peak areas of PLLA and SOY were used to determine the concentration of SOY from the calibration curve.

Morphology Observation. The blend morphology was observed using both a JEOL 1210 transmission electron microscope and a JEOL 6500 scanning electron microscope operating at accelerating voltages of 120 and 5 kV, respectively. The middle section of a specimen was cryomicrotomed (Ultracut Microtome, Reichert) using a diamond knife at −150 °C. For transmission electron microscopy (TEM) micrographs, thin slices with a thickness of 80 Å were collected on 400 mesh copper grids using an eyelash and stained with vapor from a 4% aqueous solution of osmium tetroxide (OsO_4) for 30 min. The PI and SOY domains were preferentially stained. In TEM images, PI appears dark, SOY gray, and PLLA white. For scanning electron microscopy (SEM) micrographs, a polished surface of the specimen was coated with platinum of approximately 50 Å thickness. The SOY droplets were usually removed from the surface during the microtoming process because of the weak adhesion between the PLLA and SOY domains and thus were observed as holes in the SEM images. Phase-inverted samples were left at ambient temperature for a couple of months until the SOY matrix became hard enough to microtome. Staining with OsO_4 was attempted likewise to give a contrast between the SOY and PLLA domains. In the SEM images on the phase-inverted samples, the PLLA droplets appear dark while the SOY phases appear white.

Image Analysis. Image analysis of the SEM micrographs was conducted using *ScionImage* software. The cross-sectional area A_i of each individual particle i was measured and converted into an equivalent diameter $D_i = 2(A_i/\pi)^{1/2}$ of a sphere. The volume-average diameter D_v was calculated by

$$D_v = \frac{\sum_i^n D_i^3}{\sum_i^n D_i^2} \quad (2)$$

where $n = 100-500$. The volume-average diameter is used because it places more weight on the larger particles than the number-average diameter. No further correction of D_i was made for the underestimation of D_i because of the two-dimensional projection of the sphere. Additionally, particles of a size too small to be observed at the magnification chosen have been neglected.

Differential Scanning Calorimetry (DSC). DSC analysis (TA Instruments Q1000 under nitrogen gas at a scan rate of 10 °C/min from 0 to 220 °C) was used to determine the glass transition temperature of the PLLA postblending.

RESULTS AND DISCUSSION

Determination of the Flory−Huggins Interaction Parameter χ. Cloud-point data were obtained from PLLA/SOY and PLLA/PI binary blends following the procedure described in the Supporting Information. The characteristics of the polymers used in the measurements are given in Table S1 in the Supporting Information. The temperatures at which the blends transitioned from phase-separated to homogeneous (as indicated by a transition from cloudy to clear) are given as a function of the PLLA concentration in Figures S1 and S2 in the Supporting Information. The expressions for the theoretical binodal curves, determined from the Flory−Huggins free-energy expression (38, 39), were fit to the data with χ as an adjustable parameter. The temperature dependencies of $\chi_{SOY/PLLA}$ and $\chi_{PI/PLLA}$ are given in Figure 1. Independent measurements of the χ parameters are in good agreement with one another. Direct evaluation of χ from cloud-point measurements was not successful in the case of PI/SOY because they were always completely miscible at room temperature up to a PI molecular weight of 41 kg/mol. Blends were not prepared with PI homopolymers of larger molecular weight. Instead, we provide a crude estimate of $\chi_{PI/SOY}$, relying upon the self-consistency of solubility parameters δ_i of component i, following eq S2, assuming that $\chi_{ij} \sim v(\delta_i - \delta_j)^2$ is satisfied for all components. The predicted $\chi_{PI/SOY}$ is shown as a dashed line in Figure 1. χ

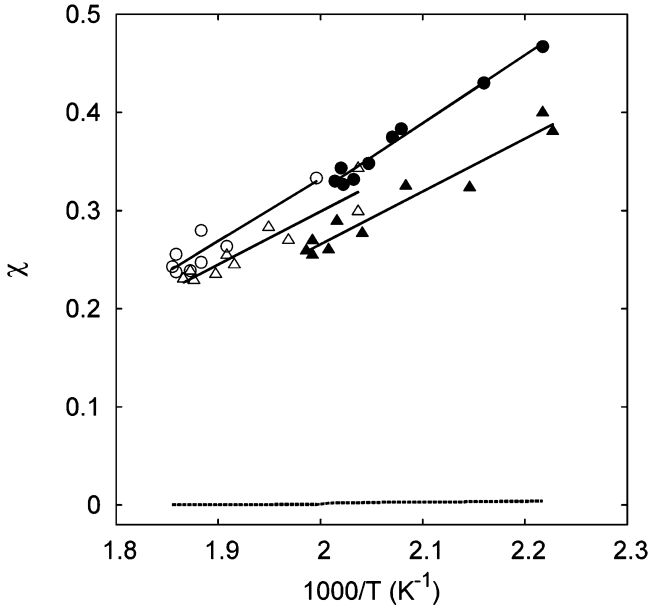

FIGURE 1. Flory–Huggins interaction parameters, $\chi_{PI/PLLA}$ (○, PI2/PLLA3; ●, PI1/PLLA1), $\chi_{SOY/PLLA}$ (Δ, SOY/PLLA4; ▲, SOY/PLLA2), and $\chi_{PI/SOY}$ (- - -) as a function of inverse temperature (solid curves are the fit of $\chi = A/T + B$ to the data).

Table 2. Summary of the Flory–Huggins Interaction Parameters [$\chi = A/T$ (K) + B][a]

binary blends	A	B	χ (190 °C)	temperature range (°C)
SOY/PLLA1	538	−0.810	0.35	176–231
SOY/PLLA2	538	−0.778		218–263
PI1/PLLA3	691	−1.060	0.43	178–224
PI2/PLLA4	633	−0.934		228–266
PI/SOY [b]	12.5	−0.023	0.004	178–263

[a] Based on a reference volume of 163 Å^3. [b] Predicted assuming a self-consistency of solubility parameters.

values for all blends studied are summarized as a functional form of $\chi = A/T + B$ in Table 2.

Binary Melt Blending of SOY and PLLA. High-molecular-weight PLLA (M_n = 54 kg/mol; PDI = 1.73) and SOY were mixed in the DACA mixer, with the concentration of SOY varying from 10 to 30 wt %. After mixing, a substantial amount of pure SOY was always left in the bottom of the DACA chamber. A calibration curve was prepared for SEC analysis to determine the concentration of SOY in the final blends. The raw SEC data are shown in Figure 2a. The percentage given above each curve is the calculated percentage of SOY in each blend after melt mixing. Regardless of the starting concentration, the final values are all around 6 wt % SOY (±1 wt %). In Figure 2b, SEM image shows SOY droplets with a volume-average diameter of 9.6 ± 7.0 μm due to the large interfacial tension between SOY and PLLA. The cryomicrotoming process resulted in the removal of SOY from the sample, leaving holes that are seen as dark circles surrounded by bright rings. The size and amount of the SOY phase were more or less consistent under various experimental conditions such as the mixing speed, feeding rate of SOY, and total mixing time.

In principle, it is extremely difficult to efficiently blend SOY and PLLA under external flow because of their large mismatch in viscosity. For instance, the viscosity ratio (at 190 °C) of SOY (η_d) to PLLA (η_m) is $\eta_d/\eta_m \sim 10^{-5}$ at $\dot{\gamma} = 50$ s^{-1} in simple steady shear. Although eq 1 is not explicitly applicable to blends with a viscosity ratio far from 1, it is predicted that at a critical concentration of SOY there should be a phase-inversion point in the PLLA/SOY binary blend. When SOY is added at a concentration of less than the phase-inversion point, the morphology of the blend consists of SOY particles in a PLLA matrix. As the concentration of SOY is increased, eventually the phase-inversion point will be reached, above which the expected morphology is PLLA droplets in a SOY matrix. One explanation for the inability to incorporate more than 6 wt % SOY in the blend is that the phase-inversion point occurs at 6 wt % SOY. The unincorporated SOY visibly leaks out of the mixer during the extrusion of the sample and also after the mixer was opened up. However, such a phase-inverted structure was not explicitly observed, presumably because of the fact that the stress acting on the PLLA particles during mixing might not be high enough to break up PLLA into smaller domains (due to the low SOY viscosity). One of the difficulties in compounding a low-viscosity fluid into a polymer matrix is that the fluid has the tendency to accumulate in the high-shear-rate zones of the mixer, such as at the walls of the mixing channel (40). It is likely that the excess SOY is simply distributed around the mixing chamber, as evidenced by the leakage of SOY upon removal of the sample. As a result, once the critical value of 6 wt % SOY is added to the mixer, additional SOY does not have an effect on the final morphology or concentration of SOY incorporated into the blend. It is worth noting that, based upon DSC experiments, no plasticization of the PLLA matrix was observed in any SOY-containing blend that we examined.

PLLA/SOY/ILLA Ternary Blends. In the ternary blends, the emulsifying efficacy of the ILLA block copolymer was controlled by varying the PLLA block molecular weight at fixed PI block molecular weight. Ternary blends of PLLA/SOY/ILLA were prepared by melt blending 5 wt % block copolymer (based on the total blend weight) with the PLLA pellets and subsequently adding 5–20 wt % SOY based on the total blend weight. The morphologies of representative ternary blends with a wt % of SOY (w_{SOY}) = 5 wt % are shown in Figure 3. Asymmetric copolymers with $f_{PLLA} \geq 0.74$ led to only slight decreases in the SOY droplet size compared to the binary blend. However, the droplet size was dramatically reduced as f_{PLLA} decreased until f_{PLLA} reached 0.57. When f_{PLLA} further decreased, phase inversion occurred within a narrow range of f_{PLLA} between 0.55 and 0.57 (Figure 3d). At the phase-inversion point, the majority PLLA became the dispersed phase and the minority SOY phase became the continuous phase, resembling a foamy network structure. The SOY matrix does not provide enough mechanical strength so that the phase-inverted composites were very brittle (and crumbled when handled). Figure 3d also reveals that the majority PLLA droplets were deformed into poly-

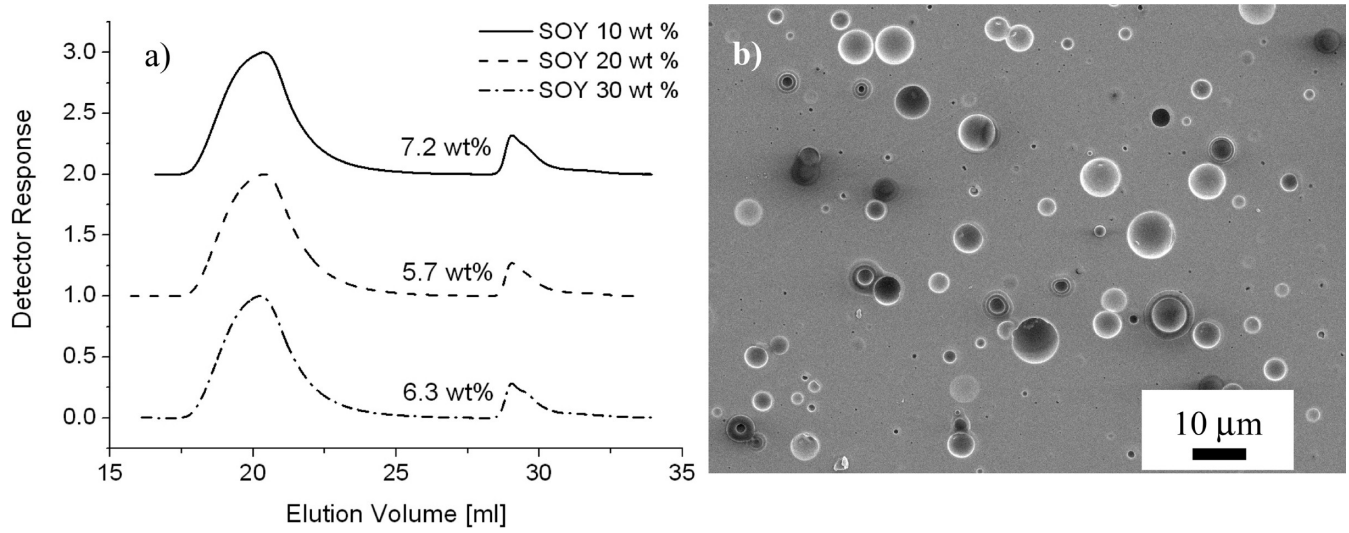

FIGURE 2. (a) SEC data of binary blends for three different initial amounts of SOY: 10, 20, and 30 wt %. (b) SEM micrograph of a binary 80% PLLA/20% SOY blend, which contained 5.7 wt % of SOY after mixing.

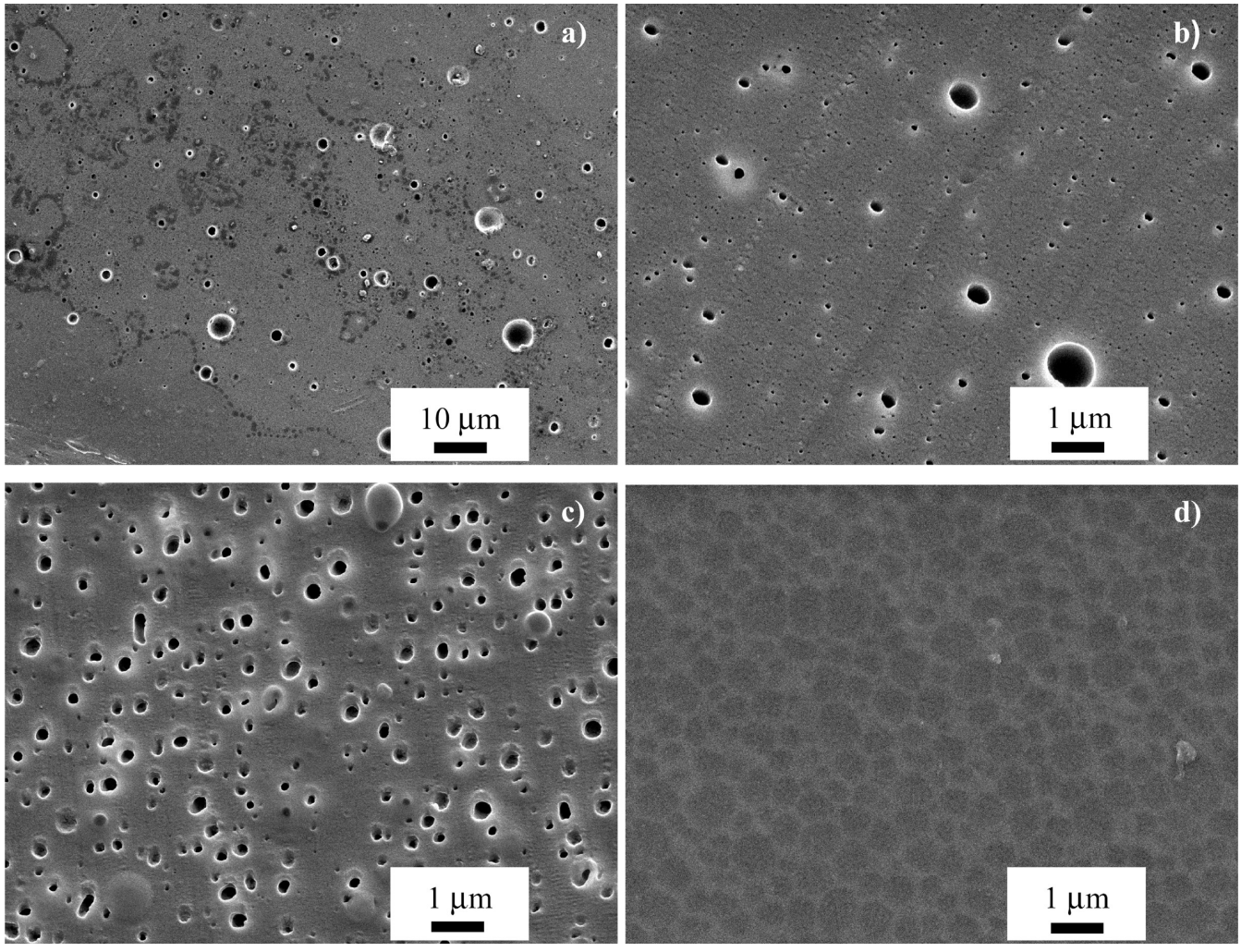

FIGURE 3. SEM micrographs of ternary blends of PLLA (90 wt %)/SOY (5 wt %)/ILLA (5 wt %): (a) ILLA74; (b) ILLA70; (c) ILLA59; (d) ILLA55. The PLLA phase appears dark in the phase-inverted blend (d) because of staining with OsO_4.

hedra, separated by thin SOY layers, because of the packing constraints of a dispersed phase with volume fraction >0.74, the maximum volume fraction of closely packed hard spheres.

As the amount of SOY was increased to 10 and 15 wt %, similar trends in blend morphology were observed. The SEM images of these blends are shown in Figures S3 and S4 of the Supporting Information. The average diameter of drop-

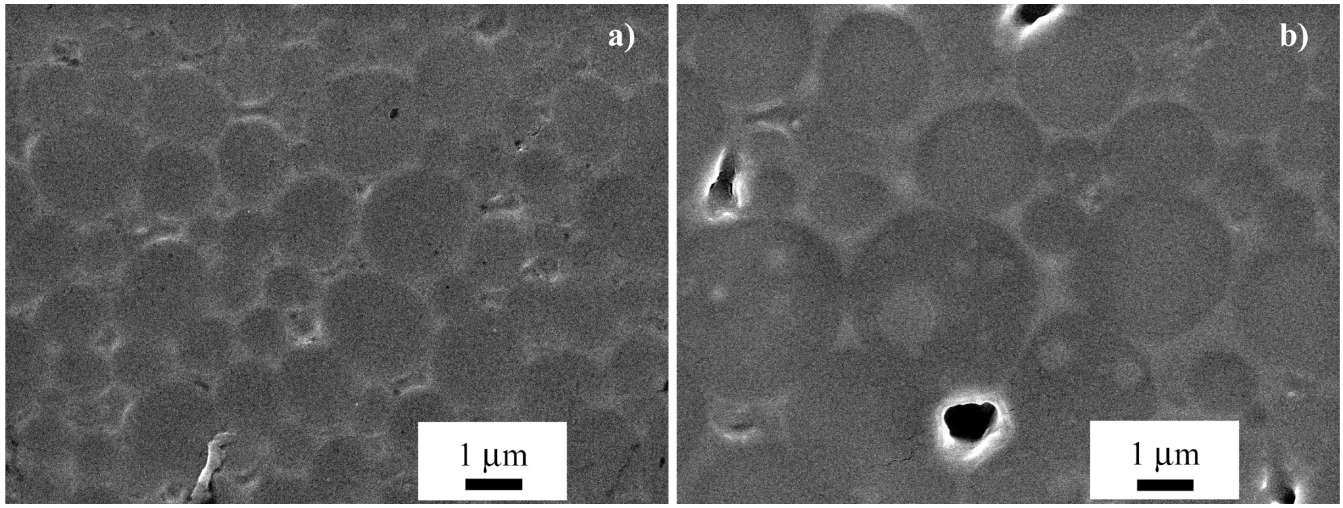

FIGURE 4. SEM micrographs of phase-inverted ternary blends: (a) 85% PLLA/10% SOY/5% ILLA59; (b) 80% PLLA/15% SOY/5% ILLA63.

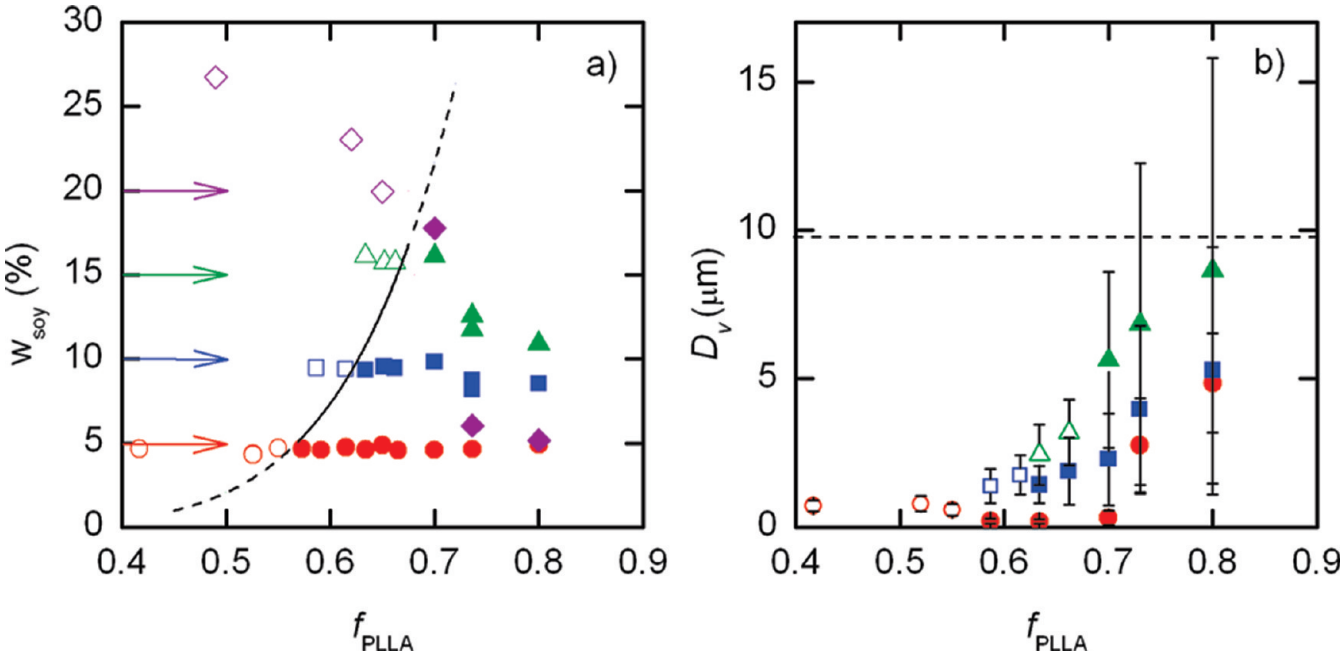

FIGURE 5. (a) Weight percent of SOY (w_{SOY}) incorporated and (b) volume-average drop diameter (D_v) as a function of f_{PLLA} for ternary blends. For both figures, the data symbols indicate the initial weight percent of SOY added to the mixer: 5% (●), 10% (■), 15% (▲), and 20% (♦). Data for 20% SOY are not shown in Figure 5b. Open symbols indicate phase-inverted samples, and solid symbols indicate normal samples. In Figure 5a, the arrows indicate the wt % SOY initially added to the blend for each data set. The phase-inversion boundary is indicated as a solid curve. Extrapolations to the phase-inversion boundary are indicated as dashed curves. The data points for 5 and 20% SOY are overlapping at $f_{PLLA} = 0.8$. The phase-inverted blends containing initially 20 wt % SOY began to show signs of sedimentation of the PLLA particles immediately upon removal from the mixer. The measurements of the weight percent of SOY incorporated were conducted on the top portion of the sample, resulting in w_{SOY} values of 20 wt % or greater. In Figure 5b, the dashed line indicates the average drop size of the binary blends in the absence of block copolymer.

lets increased as the SOY concentration increased and the phase-inversion point moved to higher f_{PLLA} (roughly 0.62 and 0.68 for 10 and 15 wt % SOY, respectively). As the packing constraint was released with an increasing volume fraction of SOY, the original spherical shape was recovered in the phase-inverted blends as shown in Figure 4. It was also observed that some smaller-diameter SOY droplets were included within the PLLA droplets with 15 wt % SOY. At 20 wt % (i.e., 26 vol %) SOY, the phase-inverted blends with $f_{PLLA} < 0.70$ became very viscous at room temperature because of sedimentation of the PLLA droplets, thus preventing direct observation of the morphology. The thermal stability of three ternary blends (85% PLLA/10% SOY/5% ILLA) was probed by annealing the blends at 190 °C for 1 h. In all three cases, there was no evidence of coarsening of the dispersed particle phase. The SEM images of the blends after annealing are shown in Figure S5 of the Supporting Information.

Figure 5a summarizes the weight fraction of SOY (w_{SOY}) actually incorporated into the ternary blends as a function of the block copolymer composition f_{PLLA} (at 5 wt % block copolymer). In contrast to the binary blends, nearly all of the SOY could be emulsified in the final mixtures at $f_{PLLA} <$ 0.7. In blends containing ILLA block copolymers with f_{PLLA}

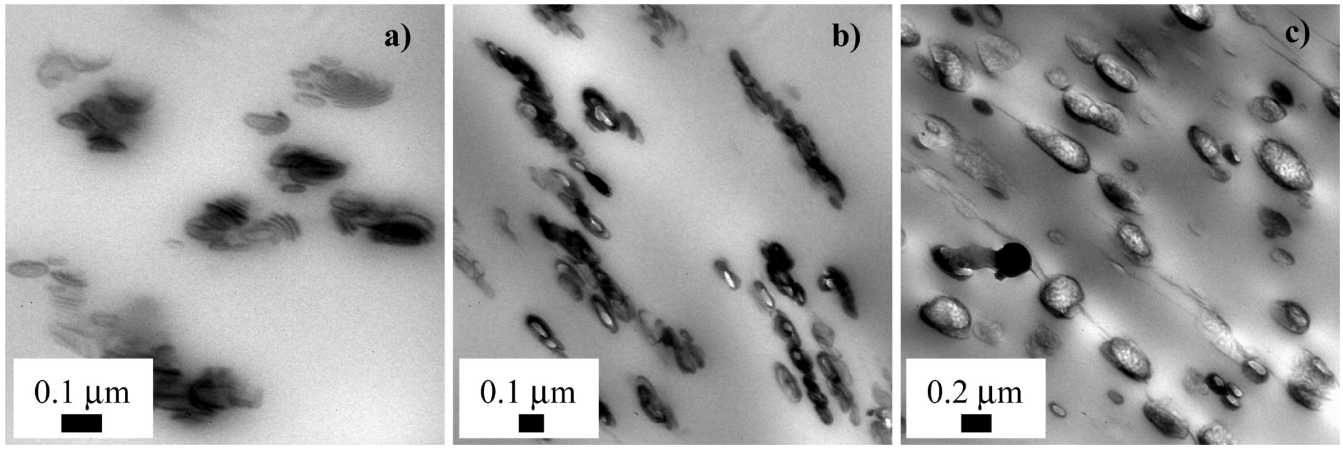

FIGURE 6. TEM micrographs of ternary melt blends of PLLA/SOY/ILLA63 containing the following SOY concentrations: (a) 0 wt %; (b) 2.0 wt %; (c) 3.9 wt %.

> 0.7, SOY was partially included, indicating the reduced emulsifying capability of the block copolymer. Only when the initial concentration of SOY was 5 wt % (i.e., below the proposed phase-inversion weight fraction in binary blends) could all of the SOY be incorporated regardless of the block copolymer composition.

The phase-inversion boundary suggested by SEM micrographs is indicated by the solid curve in Figure 5a. An additional indication of phase inversion during melt blending was a sudden drop in the mixing torque and normal force. The phase-inversion point monotonically shifted to higher f_{PLLA} with increasing w_{SOY}. Only block copolymers with f_{PLLA} below a critical value are able to stabilize the phase-inverted morphology. Above this critical value, the morphology reverts to the normal morphology of SOY droplets in a PLLA matrix.

In Figure 5b, the droplet size is plotted as a function of f_{PLLA}. The droplet size decreases and becomes more uniform with decreasing f_{PLLA}. At constant blending conditions (such as the temperature, mixing rate, and mixing time) (26, 27), the droplet diameter primarily depends on the interfacial tension between SOY and PLLA and the level of droplet coalescence during mixing (28). The concentration of free block copolymer chains, related to the critical micelle concentration of the block copolymer, is a function of the core block molecular weight, which is held constant in this experiment (41). To suppress the SOY droplet coalescence, a larger PLLA block should be more efficient at suppression of coalescence because of steric hindrance between block copolymer brushes adsorbed at the matrix/droplet interface (29). In Figure 5b, as f_{PLLA} decreases, the molecular weight of the PLLA block also decreases, but this results in a decrease in the droplet size. The opposite would be expected if droplet coalescence was a dominant factor. Therefore, the most likely explanation for the trend in the droplet size is ascribed to the effect of the block copolymer on reducing the interfacial tension of the system. In ref 34, a quadratic dependence of the interfacial tension on the block copolymer composition was measured, and this qualitatively agrees with the dependence of the droplet diameter on the block copolymer composition observed in Figure 5b.

Both the composition of the block copolymer and the concentration of SOY in the blend concomitantly influence the mean curvature of the block-copolymer-laden interface by tuning the stretching energy of the PLLA block and the ability of the PI brush to emulsify SOY. The elasticity of the "dry" PLLA brush with a smaller chain length than the PLLA homopolymer is primarily governed by the block length. It plays a role in restricting the indefinite swelling of the PI block due to the penetration of SOY. Thus, there is an optimal block copolymer composition in which a balance point is achieved and the osmotic pressure difference across the interface is zero. With decreasing f_{PLLA} toward the balance point, the spontaneous curvature of the micelle also decreases, causing not only a reduction in the interfacial tension, which promotes the breakup of SOY domains, but also an increase in the micelle size, which narrows the size distribution of SOY droplets. Beyond the balance point, the curvature changes in sign and micellization becomes more favorable in the minority SOY domain. This balance point is evidenced by the decrease in the mean particle size shown in Figure 5b.

Ternary blends can incorporate more SOY than binary blends, even beyond the amount predicted by eq 1, because the block copolymer micelles emulsify SOY in the core and swell until the equilibrium spontaneous curvature is achieved. Provided that all molecular characteristics of the homopolymers are known, the composition of the block copolymer determines the maximum amount of SOY in the micelle core. If more SOY is added than the maximum micelle core swelling capacity, the excess SOY phase separates into macroscopic SOY domains in the PLLA matrix. In the ternary PLLA/SOY/ILLA blends, it appears that, at $f_{PLLA} > 0.7$, the emulsifying capability of micelles is not enough to incorporate all SOY added to the blend, leading to the reduction of w_{SOY} below the initial amounts in Figure 5a.

To better understand the swelling behavior of the copolymer micelles during melt blending, three samples were prepared by sequentially adding SOY to the PLLA homopolymer premixed with 5 wt % ILLA63. In contrast to the typical existence of spherical micelles, Figure 6a shows that the block copolymer forms irregular lamellar phases

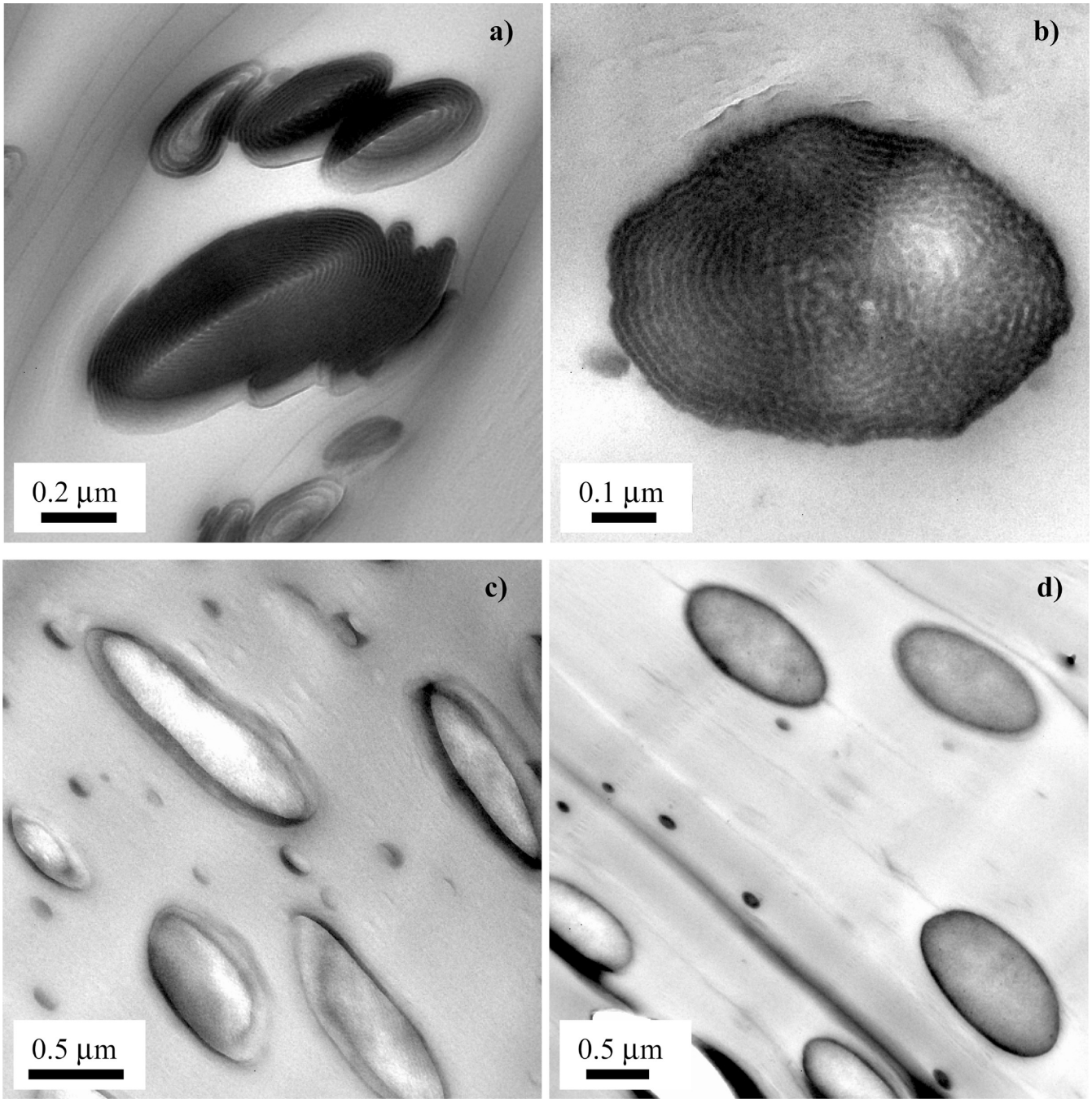

FIGURE 7. TEM micrographs of solution-blended PLLA/SOY/ILLA59 containing the following SOY concentrations: (a) 0 wt %; (b) 2 wt %; (c) 5 wt %; (d) 10 wt %.

possibly because of the considerably large Flory–Huggins interaction parameter between PI and PLLA. These lamellae swell by absorbing SOY (Figure 6b) and show characteristic internal structures (Figure 6c).

Morphology of Ternary PLLA/SOY/ILLA Blends Prepared by Solution Blending. The swelling behavior of the block copolymer was investigated in the absence of external flow. Ternary blends of PLLA/SOY/ILLA59 (containing 5 wt % of the block copolymer) were solvent-cast from chloroform. The SOY concentration was varied from 0 to 10%. The blends were flame-sealed in glass ampules and annealed in an oil bath at 190 °C for 3 h. The blend morphology is shown as a function of the SOY concentration in Figure 7. Similar to Figure 6a, a pure block copolymer forms a lamellar phase in the PLLA matrix. In the absence of shear, however, the lamellae maintained a well-defined oblate-spheroidal onion structure. This onion structure has been observed previously in the strongly segregated system of an A–B diblock copolymer blended with an A homopolymer in which the number of repeat units, N_{AB}, of the A–B diblock copolymer is much smaller than that of the A homopolymer, N_A (42). SCFT predicts that the interaction between isolated block copolymer monolayers becomes attractive if $N_A/N_{AB} > 1$ and homopolymers between copolymer brushes are expelled as copolymer monolayers approach to form dense multilayers (43, 44). Other block copolymer morphologies in the PLLA

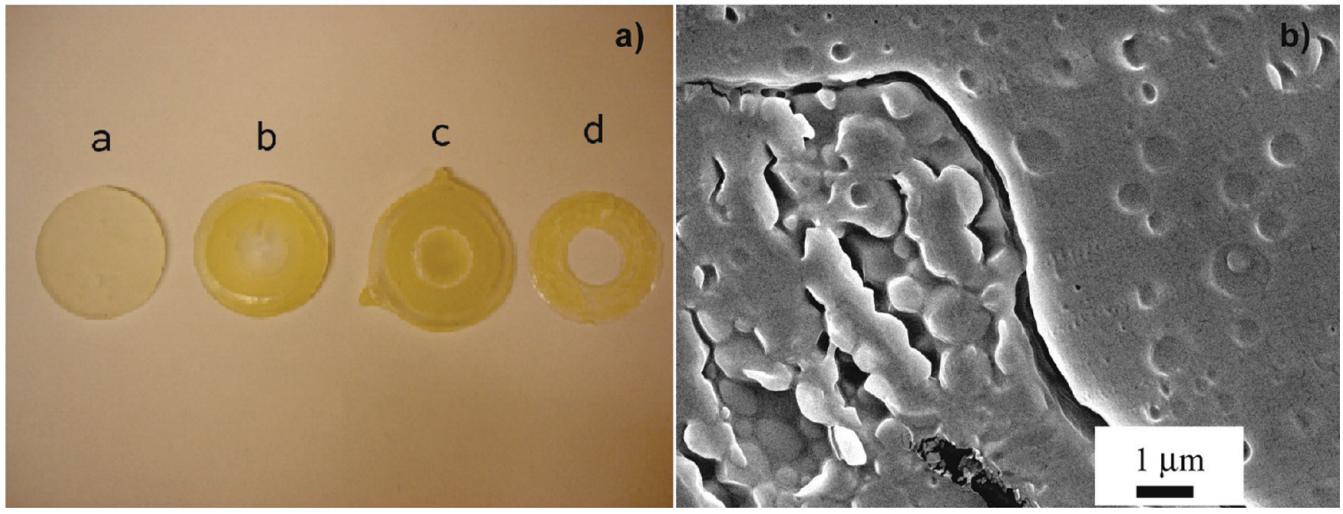

FIGURE 8. (a) 90% PLLA/5% SOY/5% ILLA55 preshear (sample a), under shear in a cone-and-plate geometry at $\dot{\gamma} = 20\ s^{-1}$ (sample b), and under shear in a parallel-plate geometry at $\dot{\gamma} = 200\ s^{-1}$ (sample c). 80% PLLA/15% SOY/5% ILLA66 under shear in a cone-and-plate geometry at $\dot{\gamma} = 200\ s^{-1}$ (sample d). Sample c exhibits localized phase inversion (with a rim forming at a local shear rate of $\dot{\gamma} = 70\ s^{-1}$), and sample d is phase-inverted throughout the entire sample. (b) SEM image of sample c near the phase-inversion boundary. The disk center is located toward the right top corner of the image.

matrix, observed from our solution-blending studies using block copolymers of varying composition, are given in the Supporting Information (Figure S6).

As w_{SOY} increased to 2 wt %, SOY preferentially swelled the PI domains and destroyed the onion layers (Figure 7b). The onion structure has disappeared at $w_{SOY} = 5$ wt %, leaving the highly swollen SOY droplets as shown in Figure 7c. The highly enlongated SOY domains might be artificially produced during the TEM sample preparation because they appeared mostly spherical in Figure 3c. With 10 wt % SOY, the SOY droplets further grew in size similar to dispersed phases ordinarily observed in ternary blends. It is important to note that, in the presence of ILLA59, the blend containing 10 wt % SOY formed a phase-inverted structure during melt blending (Figure 5a), whereas phase inversion was not observed in solvent-cast blends regardless of the amount of SOY or the block copolymer composition.

Shear-Induced Phase Inversion. Ternary solution blends were exposed to steady shear to elucidate the effect of shear flow on the observation of phase inversion. A blend containing 90% PLLA/5% SOY/5% ILLA55 was found in the phase-inversion region in Figure 5a under melt-mixing conditions but was not phase-inverted during solvent casting. This blend was sheared beginning at $\dot{\gamma} = 0.1\ s^{-1}$ up to $200\ s^{-1}$ in either parallel-plate or cone-and-plate geometries. The shear rate was gradually increased every 15 s. We expected that a critical shear rate would exist at which the steady-shear viscosity substantially drops at the onset of the phase inversion. However, such a critical shear rate was not detected in dynamic mechanical analysis because the phase inversion was preceded by an edge failure at $\dot{\gamma} = 10-20\ s^{-1}$. When a maximum $\dot{\gamma} = 20\ s^{-1}$ was applied (sample b, Figure 8a) using a cone-and-plate geometry, there was no evidence of phase inversion in spite of the edge failure. However, when the shear rate was increased up to $\dot{\gamma} = 200\ s^{-1}$ by employing a parallel-plate geometry, phase inversion was identified as a white rim in the sample near a region corresponding to a local shear rate of $\dot{\gamma} \sim 70\ s^{-1}$ (sample c, Figure 8a). Beyond this region, the disk body beneath the sample surface touching the metal plate was torn away because of edge failure. A blend containing 80% PLLA/15% SOY/5% ILLA66, also in the phase-inverted region in Figure 5a and not phase-inverted under solvent casting, was sheared at $\dot{\gamma} = 200\ s^{-1}$ in the cone-and-plate geometry (sample d, Figure 8a). In this case, the entire sample underwent phase inversion because of a constant shear rate across the sample in this geometry. In Figure 8b, an SEM image is shown of sample c (Figure 8a) at the boundary between the phase-inverted and non-phase-inverted regions.

The phase-inversion phenomena observed in the PLLA/SOY/ILLA blends cannot be attributed to thermodynamics alone. When blends were prepared via solution casting, phase inversion was not observed. It was only in the presence of external forces that phase inversion occurred, both in the DACA mixer and during the rheology experiments. Inversion of the micelle configuration through modification of the block copolymer composition does not necessarily result in the reversal of the macroscopic domains. The observation of phase inversion has been the result of the above-described thermodynamic phenomena in combination with shear forces, as qualitatively predicted by eq 1.

There are many examples in the literature in which the observation of a phase-inverted structure is dependent on thermodynamic and/or kinetic factors. In ternary blends of two homopolymers and a diblock copolymer, phase inversion has been reported to be induced by an imbalance of the swelling power of the two diblock copolymers (45, 46) as well as the solvent quality during solvent casting (47). High internal phase emulsions, water/oil and organic/organic mixtures with structures analogous to those of the phase-inverted structures discussed in this paper, are obtained under a narrow range of conditions that depend on the presence of high shear forces, a suitable mixing sequence, and surfactant efficiency (48–51). The structure of foams

consisting of gas bubbles trapped in thin liquid layers of water and surfactant can depend on factors such as the gas velocity during the foam preparation and the thermodynamic properties of the surfactant (52−54). It is possible to consider the stabilization of the phase-inverted structure in PLLA/SOY/ILLA blends in a similar manner. The shear forces during melt blending in a DACA mixer result in phase inversion of the ternary blends. The block copolymer stabilizes the phase-inverted structure, which otherwise reverts to a non-phase-inverted morphology in the absence of an appropriate block copolymer.

CONCLUSIONS

Renewable PLLA/SOY blends were prepared using a melt mixer. Because of the large incompatibility between PLLA and SOY, the emulsifying effect of ILLA block copolymers on the blend morphology was probed. Upon the addition of SOY, the block copolymer micelles swelled by absorbing SOY in the core. Consequently, the incorporation of SOY in the ternary blends dramatically increased compared to that of the binary blends. The droplet size of the minority SOY domains was monotonically reduced with a decreasing fraction of PLLA in the block copolymer (f_{PLLA}) until phase inversion occurred between SOY and PLLA. The phase inversion occurred at a critical value of f_{PLLA}, and that value was also dependent on the concentration of SOY in the mixture. However, when identical blends were prepared with solvent-casting techniques, phase inversion was not observed, at any value of f_{PLLA}. Thus, phase inversion was found to be dependent on both thermodynamic and kinetic factors. The design of the block copolymer is essential in tuning the morphology of PLLA/SOY/ILLA blends. The appropriate choice of the block copolymer in PLLA/SOY/ILLA blends can (1) prevent phase inversion, (2) minimize the size of the SOY droplets, and (3) allow for the complete incorporation of SOY (up to 20 wt %) during mixing. Collectively, these results pave the way for the future development of SOY/PLLA blends.

Acknowledgment. The authors thank Toyota Motor Corp. for financial support. Parts of this work were carried out in the University of Minnesota IT Characterization Facility, which receives partial support from the NSF through the NNIN program.

Supporting Information Available: Determination of Flory−Huggins interaction parameters with cloud-point measurements, morphology of PLLA/SOY/ILLA blends with varying amounts of SOY, effect of annealing on the morphology of PLLA/SOY/ILLA blends, and micelle structures of block copolymers within the PLLA matrix. This material is available free of charge via the Internet at http://pubs.acs.org.

REFERENCES AND NOTES

(1) Flieger, M.; Kantorova, M.; Prell, A.; Rezanka, T.; Votruba, J. *Folia Microbiol.* **2003**, *48*, 27–44.
(2) Mohanty, A. K.; Misra, M.; Drzal, L. T. *J. Polym. Environ.* **2002**, *10*, 19–26.
(3) Sudesh, K.; Iwata, T. *Clean-Soil Air Water* **2008**, *36*, 433–442.
(4) Young, J. L.; Woerderman, D. L.; Selling, G. W. *J. Biobased Mater. Bioenergy* **2007**, *1*, 171–176.
(5) Yu, L.; Dean, K.; Li, L. *Prog. Polym. Sci.* **2006**, *31*, 576–602.
(6) Garlotta, D. *J. Polym. Environ.* **2001**, *9*, 63–84.
(7) Sodergard, A.; Stolt, M. *Prog. Polym. Sci.* **2002**, *27*, 1123–1163.
(8) Li, S. M. *J. Biomed. Mater. Res.* **1999**, *48*, 342–353.
(9) Anderson, K. S.; Schreck, K. M.; Hillmyer, M. A. *Polym. Rev.* **2008**, *48*, 85–108.
(10) Anderson, K. S.; Hillmyer, M. A. *Polymer* **2004**, *45*, 8809–8823.
(11) Li, Y. J.; Shimizu, H. *Macromol. Biosci.* **2007**, *7*, 921–928.
(12) Kim, K. S.; Chin, I. J.; Yoon, J. S.; Choi, H. J.; Lee, D. C.; Lee, K. H. *J. Appl. Polym. Sci.* **2001**, *82*, 3618–3626.
(13) Hiljanen Vainio, M.; Varpomaa, P.; Seppala, J.; Tormala, P. *Macromol. Chem. Phys.* **1996**, *197*, 1503–1523.
(14) Noda, I.; Satkowski, M. M.; Dowrey, A. E.; Marcott, C. *Macromol. Biosci.* **2004**, *4*, 269–275.
(15) Chen, G. X.; Kim, H. S.; Kim, E. S.; Yoon, J. S. *Polymer* **2005**, *46*, 11829–11836.
(16) Ali, F.; Chang, Y. W.; Kang, S. C.; Yoon, J. Y. *Polym. Bull.* **2009**, *62*, 91–98.
(17) Choi, J. S.; Park, W. T. *Macromol. Symp.* **2003**, *197*, 65–76.
(18) Brostrom, J.; Boss, A.; Chronakis, L. S. *Biomacromolecules* **2004**, *5* (3), 1124–1134.
(19) Guner, F. S.; Yagci, Y.; Erciyes, A. T. *Prog. Polym. Sci.* **2006**, *31*, 633–670.
(20) Meier, M. A. R.; Metzger, J. O.; Schubert, U. S. *Chem. Soc. Rev.* **2007**, *36*, 1788–1802.
(21) Sharma, V.; Kundu, P. P. *Prog. Polym. Sci.* **2006**, *31*, 983–1008.
(22) Metzger, J. O.; Bornscheuer, U. *Appl. Microbiol. Biotechnol.* **2006**, *71*, 13–22.
(23) Wu, S. H. *J. Appl. Polym. Sci.* **1988**, *35*, 549–561.
(24) Perkins, W. G. *Polym. Eng. Sci.* **1999**, *39*, 2445–2460.
(25) Corte, L.; Leibler, L. *Macromolecules* **2007**, *40*, 5606–5611.
(26) Wu, S. H. *Polym. Eng. Sci.* **1987**, *27*, 335–343.
(27) Favis, B. D.; Chalifoux, J. P. *Polym. Eng. Sci.* **1987**, *27*, 1591–1600.
(28) Paul, D. R.; Bucknall, C. B. *Polymer Blends*; Wiley: New York, 2000.
(29) Sundararaj, U.; Macosko, C. W. *Macromolecules* **1995**, *28*, 2647–2657.
(30) Potschke, P.; Paul, D. R. *J. Macromol. Sci., Polym. Rev.* **2003**, *C43*, 87–141.
(31) Smith, A. P.; Ade, H.; Smith, S. D.; Koch, C. C.; Spontak, R. J. *Macromolecules* **2001**, *34*, 1536–1538.
(32) Jeon, H. S.; Nakatani, A. I.; Hobbie, E. K.; Han, C. C. *Langmuir* **2001**, *17*, 3087–3095.
(33) Lazo, N. D. B.; Scott, C. E. *Polymer* **2001**, *42*, 4219–4231.
(34) Chang, K.; Morse, D. C. *Macromolecules* **2006**, *39*, 7397–7406.
(35) Chang, K.; Macosko, C. W.; Morse, D. C. *Macromolecules* **2007**, *40*, 3819–3830.
(36) Wang, Y. B.; Hillmyer, M. A. *Macromolecules* **2000**, *33*, 7395–7403.
(37) Schmidt, S. C.; Hillmyer, M. A. *Macromolecules* **1999**, *32*, 4794–4801.
(38) Flory, P. J. *J. Chem. Phys.* **1942**, *10*, 51–61.
(39) Huggins, M. L. *J. Chem. Phys.* **1942**, *46*, 151–158.
(40) Scott, C. E.; Joung, S. K. *Polym. Eng. Sci.* **1996**, *36*, 1666–1674.
(41) Alexandridis, P.; Hatton, T. A. *Colloids Surf., A* **1995**, *96*, 1–46.
(42) Koizumi, S.; Hasegawa, H.; Hashimoto, T. *Macromolecules* **1994**, *27*, 6532–6540.
(43) Thompson, R. B.; Matsen, M. W. *J. Chem. Phys.* **2000**, *112*, 6863–6872.
(44) Janert, P. K.; Schick, M. *Macromolecules* **1998**, *31*, 1109–1113.
(45) Adedeji, A.; Jamieson, A. M.; Hudson, S. D. *Macromolecules* **1995**, *28*, 5255–5261.
(46) Adadeji, A.; Jamieson, A. M.; Hudson, S. D. *Macromol. Chem. Phys.* **1996**, *197*, 2521–2538.
(47) Mezzenga, R.; Fredrickson, G. H.; Kramer, E. J. *Macromolecules* **2003**, *36*, 4457–4465.
(48) Lissant, K. J. *J. Colloid Interface Sci.* **1966**, *22*, 462–468.
(49) Mason, T. G.; Wilking, J. N.; Meleson, K.; Chang, C. B.; Graves, S. M. *J. Phys.: Condens. Matter* **2006**, *18*, R635–R666.
(50) Menner, A.; Bismarck, A. *Macromol. Symp.* **2006**, *242*, 19–24.
(51) Cameron, N. R.; Sherrington, D. C. *J. Chem. Soc., Faraday Trans.* **1996**, *92*, 1543–1547.
(52) Stone, H. A.; Koehler, S. A.; Hilgenfeldt, S.; Durand, M. *J. Phys.: Condens. Matter* **2003**, *15* (1), S283–S290.
(53) Joseph, D. D. *J. Fluids Eng. Trans. ASME* **1997**, *119*, 497–498.
(54) Guitian, J.; Joseph, D. *Int. J. Multiphase Flow* **1998**, *24*, 1–16.

AM900514V